

Entangling two levitated charged nanospheres through Coulomb interaction

Guoyao Li(李国耀) and Zhangqi Yin(尹璋琦)

Citation: Chin. Phys. B, 2024, 33 (**7**): 074205. DOI: 10.1088/1674-1056/ad3229
Journal homepage: http://cpb.iphy.ac.cn; http://iopscience.iop.org/cpb

What follows is a list of articles you may be interested in

State transfer and entanglement between two- and four-level atoms in a cavity

Si-Wu Li(李思吾), Tianfeng Feng(冯田峰), Xiao-Long Hu(胡骁龙), and Xiaoqi Zhou(周晓祺)
Chin. Phys. B, 2023, 32 (**10**): 104214. DOI: 10.1088/1674-1056/acf205

Nonreciprocal coupling induced entanglement enhancement in a double-cavity optomechanical system

Yuan-Yuan Liu(刘元元), Zhi-Ming Zhang(张智明), Jun-Hao Liu(刘军浩), Jin-Dong Wang(王金东), and Ya-Fei Yu(於亚飞)
Chin. Phys. B, 2022, 31 (**9**): 094203. DOI: 10.1088/1674-1056/ac6499

Bright 547-dimensional Hilbert-space entangled resource in 28-pair modes biphoton frequency comb from a reconfigurable silicon microring resonator

Qilin Zheng(郑骑林), Jiacheng Liu(刘嘉成), Chao Wu(吴超), Shichuan Xue(薛诗川), Pingyu Zhu(朱枰谕), Yang Wang(王洋), Xinyao Yu(于馨瑶), Miaomiao Yu(余苗苗), Mingtang Deng(邓明堂), Junjie Wu(吴俊杰), and Ping Xu(徐平)
Chin. Phys. B, 2022, 31 (**2**): 024206. DOI: 10.1088/1674-1056/ac3507

Quantum speed limit time and entanglement in a non-Markovian evolution of spin qubits of coupled quantum dots

M. Bagheri Harouni
Chin. Phys. B, 2020, 29 (**12**): 124203. DOI: 10.1088/1674-1056/abab75

Reversion of weak-measured quantum entanglement state

Shao-Jiang Du(杜少将), Yonggang Peng(彭勇刚), Hai-Ran Feng(冯海冉), Feng Han(韩峰), Lian-Wu Yang(杨连武), Yu-Jun Zheng(郑雨军)
Chin. Phys. B, 2020, 29 (**7**): 074202. DOI: 10.1088/1674-1056/ab8c3e

---

Entangling two levitated charged nanospheres through Coulomb interaction

Guoyao Li(李国耀) and Zhangqi Yin(尹璋琦)†

Center for Quantum Technology Research and Key Laboratory of Advanced Optoelectronic Quantum Architecture and Measurements (MOE), School of Physics, Beijing Institute of Technology, Beijing 100081, *China*

(Received 22 December 2023; revised manuscript received 12 February 2024; accepted manuscript online 11 March 2024)

Limited by the thermal environment, the entanglement of a massive object is extremely difficult to generate. Based on a coherent scattering mechanism, we propose a scheme to generate the entanglement of two optically levitated nanospheres through the Coulomb interaction. Two nanospheres are charged and coupled to each other through the Coulomb interaction. In this manner, the entanglement of two nanospheres is induced either under a weak/strong optomechanical coupling regime or under an ultra-strong optomechanical coupling regime. The charges, radius and distance of the two nanospheres are taken into consideration to enhance the Coulomb interaction, thereby achieving a higher degree of entanglement in the absence of ground-state cooling. The corresponding maximum entanglement can be attained as the dynamics of the system approaches the boundary between the steady and the unsteady regimes. This provides a useful resource for both quantum-enhanced sensing and quantum information processing, as well as a new platform for studying many-body physics.

Keywords: quantum entanglement, coherent scattering, Coulomb interaction

PACS: 42.50.Pq, 03.67.Mn **DOI:** 10.1088/1674-1056/ad3229

1. Introduction

Entanglement plays a pivotal role in fundamental physics, showcasing its immense potential for applications in quantum computation,[1] quantum networks[2] and measurement beyond the quantum limit.[3,4] Quantum entanglement has been proven at the atomic scale,[5–7] but generating entanglement in macroscopic systems is difficult due to increasing noise.[8] One available method is a levitated optomechanical system in which optically levitated objects have negligible contact damping thereby preserving quantum coherence from the thermal environment.[9,10] The decoherence resulting from gas molecule collisions will be smaller than that caused by photon recoil if the residual gas pressure is sufficiently low.[11–13] When the optomechanical coupling is larger than the decoherence rate it enables entanglement at a macroscopic scale.[14]

Levitated optomechanical systems, capable of optically levitating nano- and micro-objects in an ultra-high vacuum environment, have been behind many recent scientific achievements, including the ground-state cooling of motional modes,[9,15–17] strong and ultra-strong optomechanical coupling,[18–21] quantum squeezing of the motional mode,[22,23] phonon lasers,[24,25] dipole–dipole interaction between two levitated nanoparticles[26] and ultra-high sensitivity force sensing.[27,28] Extreme environmental isolation will prevent decoherence of the optically levitated object, presenting a promising pathway towards achieving quantum effects on a macroscopic scale.[29–31] Based on this, many theoretical schemes have been proposed to generate quantum entanglement of nanospheres, either with or without a cavity.[32–35] However, limited by the thermal environment, the motion of the nanosphere must be cooled to the ground state, where the effective phonon number is far below that in current experiments.[33–35] Recently, the Coulomb interaction has been experimentally demonstrated upon sympathetic cooling and squeezing of two nanospheres in a levitated optomechanical system, showing flexible control of the motional state.[22] Moreover, the dipole–dipole interaction can be shut down by tuning the polarization angle of the trapping laser.[26] This means that the Coulomb interaction of two optically levitated nanospheres can be independently controlled in a levitated cavity optomechanical system. By introducing the Coulomb interaction into a levitated optomechanical system it is possible to generate quantum entanglement on a macroscopic scale.

In this paper, we aim to prepare the entanglement of two motional nanospheres in a levitated optomechanical system, where two charged nanospheres are optically levitated and coherently coupled to an optical cavity in a high vacuum.[20,21,36] In comparison with other optomechanical systems, an optically levitated nanosphere has no contact damping. Gas molecule collisions are the main source for the damping of the motional nanospheres. When the residual gas pressure is pumped to a higher vacuum, the reduction in collisions between gas molecules and the nanosphere will allow the motional nanosphere to have an ultra-high mechanical quality factor and high isolation from the thermal environment, leading to low decoherence on the motional nanosphere. Moreover, strong, deep-strong and ultra-strong coupling can be achieved

†Corresponding author. E-mail: zqyin@bit.edu.cn

© 2024 Chinese Physical Society and IOP Publishing Ltd

within the coherent scattering mechanism.[18,21,37] In the presence of the Coulomb interaction, the steady entanglement of two charged nanospheres is available for two-mode squeezing interaction.[22,26] Compared with the scheme of Coulomb interaction without a cavity or a cavity without Coulomb interaction, ground state cooling of two nanospheres is not necessary in our scheme.[32–35] In order to achieve the maximum entanglement of two motional nanospheres in a steady state, the distance, charges and radii of the two nanospheres are investigated to enhance the Coulomb interaction. The maximum entanglement of two motional nanospheres can be generated near the boundary of the steady and unsteady regimes.

2. Model and dynamics

As shown in Fig. 1, we consider that two uniform nanospheres are optically levitated by two linearly polarized dual optical tweezers in a Fabry–Perot cavity. The cavity field is driven by the coherent scattering photons of two nanospheres. The excited cavity photon number is not sufficient to boost the cavity-enhanced optomechanical coupling. Therefore, cavity-enhanced optomechanical coupling is not considered in this paper. Moreover, the cavity-enhanced optomechanical coupling depends on the phase (ϕ) of the cavity field, which can be switched off by moving the nanosphere to the position $\sin(2\phi) = 0$. By contrast, the coherent scattering process will cast the system into the ultra-strong coupling regime or even the deep-strong coupling regime, where the coherent scattering coupling g between the cavity mode and motional mode is comparable to or larger than the motional frequency Ω.[21,37,38] As shown in Fig. 2(b), the ratio $g_1/\Omega_1 > 1$ can be achieved via the experimental parameters, which enables the system to achieve the deep-strong coupling regime.

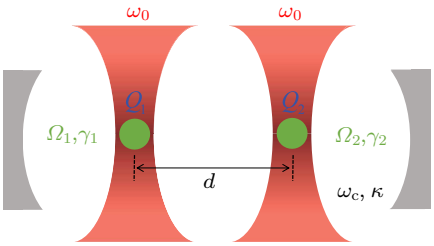


Fig. 1. Schematic diagram of the dual optical tweezers in a Fabry–Perot cavity. Two charged nanospheres are optically levitated in a cavity by the dual optical tweezers with frequency ω_0. The cavity mode is excited by the scattering photons. ω_c and κ are the cavity-mode frequency and cavity decay rate. Ω_j and γ_j are the frequency of the center-of-mass motion and damping rate in the jth nanosphere. With the charge Q_1 and Q_2 on two nanospheres separated by a distance d, the Coulomb interaction is induced between the two nanospheres.

The dual optical tweezers have the same frequency ω_0. In order to levitate the nanosphere in a high vacuum, the frequency ω_0 of the optical tweezers is detuned to the red sideband of the cavity mode. The enhancement of the anti-Stokes process will cool the motional state of the nanosphere to a low effective temperature.[14,39] This enables the motion of the nanosphere to remain dynamically stable as the residual gas pressure is pumped to a high vacuum. In this way, reduction of the stochastic collisions of gas molecules leads to a low damping rate and ultra-high mechanical quality factor.[11] In our numerical calculation, the quality factor Q of the motional nanosphere could be more than 10^7, as shown in Figs. 2(c) and 2(d). On the other hand, the ultra-high quality factor of the motional nanosphere will preserve the quantum coherence of the nanosphere in a steady state.[9] Nevertheless, generating the entanglement of two nanospheres remains challenging due to the decoherence of the thermal environment.[32] In order to generate entanglement between two nanospheres, we resort to the Coulomb interaction, where two nanospheres repel each other with charges Q_1 and Q_2. By manipulating the distance d and charge Q_i ($i = 1, 2$) of two nanospheres, the entanglement of two nanospheres could be induced via the enhanced Coulomb interaction.

With respect to the interaction picture defined by the Hamiltonian $\hat{H}_0 = \hbar\omega_0\hat{a}^\dagger\hat{a}$, the Hamiltonian for the system can be written as[20,26,36]

$$\begin{aligned}\hat{H} =\ & \hbar\Delta\hat{c}^\dagger\hat{c} + \hbar\sum_{j=1}^{2}\Omega_j\hat{b}^\dagger\hat{b} + \hbar G\left(\hat{b}_1^\dagger + \hat{b}_1\right)\left(\hat{b}_2^\dagger + \hat{b}_2\right) \\ & - \hbar\sum_{j=1}^{2} g_j\left(\hat{c}^\dagger + \hat{c}\right)\left(\hat{b}_j^\dagger + \hat{b}_j\right), \end{aligned} \tag{1}$$

where $\hat{c}^\dagger$ and $\hat{c}$ ($\hat{b}_j^\dagger$ and $\hat{b}_j$) denote the bosonic creation and annihilation operators of the cavity field [center-of-mass (CoM) motion] with the commutation relation $[\hat{a}, \hat{a}^\dagger] = 1$ ($[\hat{b}_j, \hat{b}_j^\dagger] = 1$),[40] $\Delta = \omega_c - \omega_0$ is the detuning between the cavity frequency ω_c and the frequency ω_0 of the optical tweezers and $\Omega_j = \sqrt{\frac{4\alpha_j P_j}{\pi m_j w_j^4 \varepsilon_0 c}}$ is the CoM motion frequency of the jth nanosphere. $\alpha_j = 3V_j\varepsilon_0\frac{\varepsilon_r^j - 1}{\varepsilon_r^j + 2}$ (m_j) and P_j (w_j) are the polarizability (mass) of the nanosphere and the power (beam waist) of the optical tweezers. ε_0 (ε_r^j) denotes the vacuum (relative) permittivity of the surrounding environment (nanosphere) and c is the light speed in a vacuum. With photons of the optical tweezers being scattered into the cavity field by the motional nanosphere, the cavity field is modulated by the CoM motion of the nanosphere with the coherent scattering coupling $g_j = \alpha_j E_j k y_0^j\sqrt{\frac{\omega_c}{2\hbar\varepsilon_0 V_c}}\sin(\phi)$, where $E_j = \sqrt{\frac{4P_j}{\pi w_j^2\varepsilon_0 c}}$ is the amplitude of the optical tweezers and $V_c = \pi L w_c^2/4$ is the cavity volume. L and $w_c = \sqrt{L/k}$ are the cavity length and the beam waist of the cavity field. $k = \frac{2\pi}{\lambda}$ and $y_0^j = \sqrt{\frac{\hbar}{2m_j\Omega_j}}$ are the wave number and zero-point fluctuation of the CoM mode. V_j and λ are the volume of the nanosphere and the wavelength of the optical tweezers. $G = -\frac{\chi y_0^1 y_0^2 e_0^2}{2\pi\varepsilon_0 d^3}$ is the induced Coulomb cou-

pling between two charged nanospheres, where $\chi = Q_1 Q_2$ and e_0 is the elementary charge (see Appendix A).

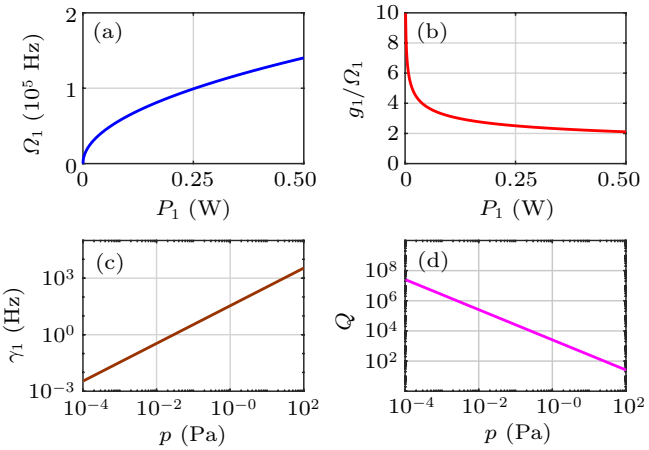


Fig. 2. The CoM motion frequency Ω_1 (a), the ratio g_1/Ω_1 (b), the damping rate γ_1 (c) and the quality factor $Q = \Omega_1/\gamma_1$ (d) as a function of the optical tweezers power P_1 and the residual gas pressure p. Parameters are as follows: wavelength of the optical tweezers $\lambda = 1064$ nm, beam waist of the tweezers in focus $w = 1$ μm, cavity length $L = 10$ mm, radius of the nanosphere $R_1 = 100$ nm, relative permittivity of the nanosphere $\varepsilon_r^1 = 2.1$, density of the nanosphere $\rho = 2200$ kg/m^3, temperature of the residual gas $T_a = 300$ K. The residual gas pressure is assumed to be $p = 10^{-4}$ Pa in (a) and (b), while the optical tweezers power $P_1 = 0.15$ W in (c) and (d).

Derived from the system Hamiltonian, the dynamics of the system can be characterized by the linear quantum Langevin equations

$$\begin{aligned}\frac{\mathrm{d}\hat{b}_1}{\mathrm{d}t} =& -\left(\mathrm{i}\Omega_1 + \frac{\gamma_1}{2}\right)\hat{b}_1 + \mathrm{i}g_1\left(\hat{c}^\dagger + \hat{c}\right) \\ & - \mathrm{i}G\left(\hat{b}_2^\dagger + \hat{b}_2\right) + \sqrt{\gamma_1}\hat{b}_1^{\mathrm{in}}, \end{aligned} \tag{2}$$

$$\begin{aligned}\frac{\mathrm{d}\hat{b}_2}{\mathrm{d}t} =& -\left(\mathrm{i}\Omega_2 + \frac{\gamma_2}{2}\right)\hat{b}_2 + \mathrm{i}g_2\left(\hat{c}^\dagger + \hat{c}\right) \\ & - \mathrm{i}G\left(\hat{b}_1^\dagger + \hat{b}_1\right) + \sqrt{\gamma_2}\hat{b}_2^{\mathrm{in}}, \end{aligned} \tag{3}$$

$$\begin{aligned}\frac{\mathrm{d}\hat{c}}{\mathrm{d}t} =& -\left(\mathrm{i}\Delta + \frac{\kappa}{2}\right)\hat{c} + \mathrm{i}g_1\left(\hat{b}_1^\dagger + \hat{b}_1\right) \\ & + \mathrm{i}g_2\left(\hat{b}_2^\dagger + \hat{b}_2\right) + \sqrt{\kappa}\hat{c}^{\mathrm{in}}, \end{aligned} \tag{4}$$

where κ is the cavity decay rate and γ_j (see Appendix B) is the damping rate of the motional nanosphere. From Eqs. (2)–(4), operators are already replaced by $\delta\hat{o} \to \hat{o}$, where $\delta\hat{o}$ represents the fluctuation of $\hat{o} = \{\hat{b}_1, b_2, \hat{c}\}$. $\hat{b}_1^{\mathrm{in}}$, $\hat{b}_2^{\mathrm{in}}$ and $\hat{c}^{\mathrm{in}}$ are the zero-mean Gaussian noises ($\langle\hat{b}_j^{\mathrm{in}}\rangle = 0, \langle\hat{c}^{\mathrm{in}}\rangle = 0$), obeying the correlation relations $\langle\hat{b}_j^{\mathrm{in}}(t)\hat{b}_j^{\mathrm{in}\dagger}(t')\rangle = (\bar{n}_{\mathrm{th}}^j + 1)\delta(t-t')$ and $\langle\hat{c}^{\mathrm{in}}(t)\hat{c}^{\mathrm{in}\dagger}(t')\rangle = \delta(t-t')$ in the high-temperature regime.[40] Here $\bar{n}_{\mathrm{th}}^j = \{\exp[\hbar\Omega_j/(k_{\mathrm{B}}T_{\mathrm{env}}^j)] - 1\}^{-1}$ is the mean thermal excitation number and k_{B} is the Boltzmann constant. Each nanosphere is considered to be coupled with its own thermal bath, at temperature T_{env}^j, leading to quantum Brownian motion for the nanosphere.[33]

Then, operators ($\hat{o}$) are decomposed to quadratures $\delta\hat{q}_j \equiv \frac{\delta\hat{b}_j + \delta\hat{b}_j^\dagger}{\sqrt{2}}$, $\delta\hat{p}_j \equiv \frac{\delta\hat{b}_j - \delta\hat{b}_j^\dagger}{\mathrm{i}\sqrt{2}}$, $\delta\hat{X} \equiv \frac{\delta\hat{c} + \delta\hat{c}^\dagger}{\sqrt{2}}$ and $\delta\hat{Y} \equiv \frac{\delta\hat{c} - \delta\hat{c}^\dagger}{\mathrm{i}\sqrt{2}}$. The corresponding Hermitian input noises are given as $\hat{q}_j^{\mathrm{in}} \equiv \frac{\hat{b}_j^{\mathrm{in}} + \hat{b}_j^{\mathrm{in}\dagger}}{\sqrt{2}}$, $\hat{p}_j^{\mathrm{in}} \equiv \frac{\hat{b}_j^{\mathrm{in}} - \hat{b}_j^{\mathrm{in}\dagger}}{\mathrm{i}\sqrt{2}}$, $\hat{X}^{\mathrm{in}} \equiv \frac{\hat{c}^{\mathrm{in}} + \hat{c}^{\mathrm{in}\dagger}}{\sqrt{2}}$ and $\hat{Y}^{\mathrm{in}} \equiv \frac{\hat{c}^{\mathrm{in}} - \hat{c}^{\mathrm{in}\dagger}}{\mathrm{i}\sqrt{2}}$. The linearized Langevin equations can be rewritten in a compact form as

$$\dot{\hat{\boldsymbol{u}}}(t) = \boldsymbol{A}\hat{\boldsymbol{u}}(t) + \hat{\boldsymbol{N}}(t), \tag{5}$$

where $\hat{\boldsymbol{u}}^{\mathrm{T}}(t) = \{\hat{q}_1(t), \hat{p}_1(t), \hat{q}_2(t), \hat{p}_2(t), \hat{X}(t), \hat{Y}(t)\}$, $\hat{\boldsymbol{N}}^{\mathrm{T}}(t) = \{\sqrt{\gamma_1}\hat{q}_1^{\mathrm{in}}, \sqrt{\gamma_1}\hat{p}_1^{\mathrm{in}}, \sqrt{\gamma_2}\hat{q}_2^{\mathrm{in}}, \sqrt{\gamma_2}\hat{p}_2^{\mathrm{in}}, \sqrt{\kappa}\hat{X}^{\mathrm{in}}, \sqrt{\kappa}\hat{Y}^{\mathrm{in}}\}$, and the drift matrix

$$\boldsymbol{A} = \begin{pmatrix} -\frac{\gamma_1}{2} & \Omega_1 & 0 & 0 & 0 & 0 \\ -\Omega_1 & -\frac{\gamma_1}{2} & -2G & 0 & 2g_1 & 0 \\ 0 & 0 & -\frac{\gamma_2}{2} & \Omega_2 & 0 & 0 \\ -2G & 0 & -\Omega_2 & -\frac{\gamma_2}{2} & 2g_2 & 0 \\ 0 & 0 & 0 & 0 & -\frac{\kappa}{2} & \Delta \\ 2g_1 & 0 & 2g_2 & 0 & -\Delta & -\frac{\kappa}{2} \end{pmatrix}. \tag{6}$$

In the regime of continuous variable systems, a levitated optomechanical system can be depicted via the Gaussian state. The initial states of the two nanospheres and the cavity field are assumed to be a thermal state and a vacuum state, respectively.[40] Both the thermal state and the vacuum state can be characterized by the first moment (displacement vector) and the second moment (covariance matrix) of the Gaussian state. Since the quantum noise $\{\hat{b}_j^{\mathrm{in}}, \hat{c}^{\mathrm{in}}\}$ is zero-mean quantum Gaussian noise and the dynamics of the system is linearized, the system is a zero-mean tripartite Gaussian state.[14] In that condition, the system can be fully depicted by a 6×6 covariance matrix $\boldsymbol{V}$, where the element of $\boldsymbol{V}$ is defined by $\boldsymbol{V}_{i,j} = \left(\langle\boldsymbol{u}_i(\infty)\boldsymbol{u}_j(\infty) + \boldsymbol{u}_j(\infty)\boldsymbol{u}_i(\infty)\rangle\right)/2$. The covariance matrix $\boldsymbol{V}$ can be calculated via the Lyapunov equation if the system reaches a steady state. With this information we can solve Eq. (5) via

$$\boldsymbol{A}\boldsymbol{V} + \boldsymbol{V}\boldsymbol{A}^{\mathrm{T}} + \boldsymbol{D} = 0, \tag{7}$$

where

$$\begin{aligned}\boldsymbol{D} =& \mathrm{diag}\left\{\frac{\gamma_1}{2}(2\bar{n}_1 + 1), \frac{\gamma_1}{2}(2\bar{n}_1 + 1),\right. \\ & \left.\frac{\gamma_2}{2}(2\bar{n}_2 + 1), \frac{\gamma_2}{2}(2\bar{n}_2 + 1), \frac{\kappa}{2}, \frac{\kappa}{2}\right\}\end{aligned}$$

denotes the correlation of different noises. In order to evaluate the steady entanglement, we introduce the logarithmic negativity[14,40]

$$E_{\mathrm{n}} = \max[0, -\ln 2\eta^-], \tag{8}$$

where $\eta^- \equiv \left\{\Sigma(\boldsymbol{V}) - [\Sigma(\boldsymbol{V}) - 4\det\boldsymbol{V}]^{1/2}\right\}^{1/2}/\sqrt{2}$ is the smallest partially transposed symplectic eigenvalue of the covariance matrix $\boldsymbol{V}$ and $\Sigma(\boldsymbol{V}) \equiv \det B_1 + \det B_2 - 2\det B_3$. B_1, B_2 and B_3 are the 2×2 block matrices of the covariance matrix

$$\boldsymbol{V} \equiv \begin{pmatrix} B_1 & B_3 \\ B_3^{\mathrm{T}} & B_2 \end{pmatrix}. \tag{9}$$

3. Effect of the Coulomb interaction on system stability

In order to generate the entanglement of two motional nanospheres in a steady state, the frequency of the optical tweezers is detuned to the red sideband of the cavity field ($\Delta \approx \Omega_1$), where the anti-Stokes process is extremely enhanced in the presence of the cavity cooling mechanism.[9,14,40] In this condition, phonons are scattered into the cavity field. The CoM motion of the nanosphere will be cooled to a low effective temperature, thereby enhancing the stability of the system in a high vacuum.[9,20,21,26] It is critical to judge the stability of the system before the discussion on entanglement. As depicted in Eq. (5), the system is characterized by linear Langevin equations. The stability of the system can be assessed by applying the Routh–Hurwitz criteria to Eq. (5), which involves solving for the eigenvalues of matrix $\boldsymbol{A}$. If these eigenvalues have negative real parts, it indicates that the system is stable in the long-time limit.[40] The corresponding stability conditions can be analytically calculated by utilizing the auxiliary Routh array, where the first column must be greater than 0. The analytical solution is too laborious to enumerate in this context. For the sake of convenience, we conducted numerical simulations to investigate the effect of Coulomb interaction on system stability.

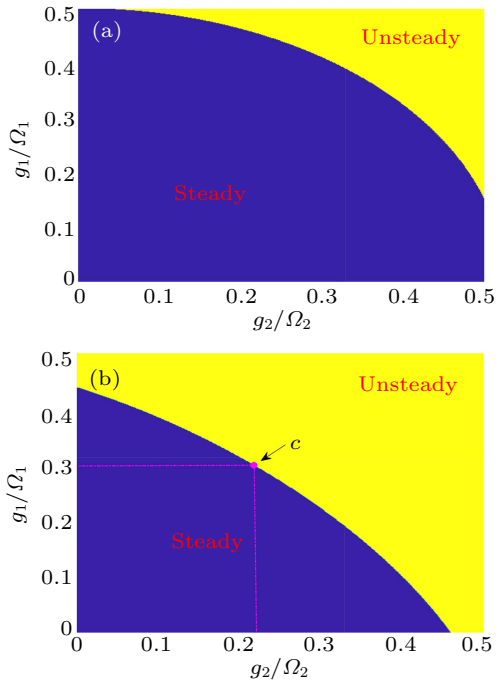


Fig. 3. The maximum real part of the eigenvalues of the matrix $\boldsymbol{A}$ as a function of the coherent scattering coupling g_j. Parts (a) and (b) depict scenarios of the absence and presence of Coulomb interaction, respectively. The blue (yellow) area indicates that the system is dynamically stable (unstable). Point c in image (b) indicates the critical condition of scattering coupling g_j on the boundary of the steady and unsteady state. Parameters are as follows: power of the first (second) optical tweezers $P_1 = 0.3$ W ($P_2 = 0.25$ W), radius of nanosphere $R_j = 100$ nm, cavity decay rate $\kappa = 0.1\Omega_1$, effective temperature of CoM mode $T_j = 0.01$ K, product of charges $\chi = Q_1 \times Q_2 = 1.2 \times 10^5$, distance of two nanospheres $d = 3\lambda$. Other parameters are the same as those in Fig. 2.

As shown in Fig. 3, the maximum real part of the eigenvalues of the matrix $\boldsymbol{A}$ is calculated with different coherent scattering couplings g_j. The blue (yellow) region indicates that the maximum real part of the eigenvalues is negative (positive), denoting that the system becomes stable (unstable) in the long-time limit. From Fig. 3, the system undergoes a transition from stability to instability as the coherent scattering coupling increases. In the presence of Coulomb interaction, the parametric area of the steady state (the blue area) exhibits a distinct reduction, as seen by comparing Figs. 3(a) and 3(b). It can be understood that the CoM motion of two nanospheres is no longer independent under Coulomb interaction. The motion of one nanosphere is affected by the motion of the other nanosphere, which produces additional forced vibrations on each nanosphere. This additional forced vibration will disturb the motion of the nanosphere, leading to the instability of two motional nanospheres. Moreover, the boundary between the stability and instability of the system is a two-dimensional curve, which is a collection of critical points with the coherent scattering couplings g_1 and g_2.

4. Coulomb interaction on entanglement

Two optically levitated nanospheres are initially in two thermal states. Entangling these two thermal states on a macroscopic scale is very difficult with large decoherence.[14] There are two available ways to generate the entanglement of two motional nanospheres as follows. One is cooling the motional nanosphere to a low effective temperature in a high vacuum. In this condition, the reduction of gas molecule collisions on the motional nanosphere results in an ultra-high mechanical quality factor and high isolation from the thermal environment. However, the effective temperature required for the generation of entanglement between two motional nanospheres is significantly lower than that achieved in current experiments.[33] Another method is to establish the direct correlation of two charged nanospheres via the Coulomb interaction. In this method, the two-mode squeezing interaction of two nanospheres will promote the generation of motional entanglement.

Figure 4(a) shows entanglement as a function of the coherent scattering coupling g_2 in the absence of the Coulomb interaction. The coherent scattering between the second nanosphere and the cavity field is assumed to be fixed in $g_1 = 0.03\Omega_1$ and $g_1 = 0.3\Omega_1$, allowing the system to achieve the weak coupling regime ($g_1/\kappa = 0.3$) and the ultra-strong coupling regime ($g_1/\Omega_1 = 0.3$).[37] Both rotating and anti-rotating wave terms have to be considered in the ultra-strong coupling regime.[38] In this condition, entanglement could be generated in the red sideband. In Fig. 4(a), there is no entanglement between two nanospheres either in the weak coupling regime or the ultra-strong coupling regime. Limited by

the heat reservoir of the other nanosphere, entanglement E_{c1} will decrease with increase in g_2, while entanglement E_{c2} will increase for the enhanced two-mode squeezing interaction between the second nanosphere and the cavity field.

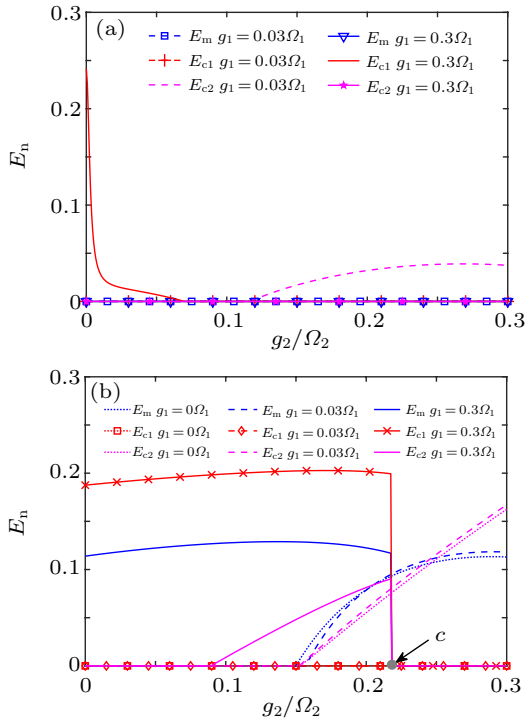


Fig. 4. Entanglement E_n as a function of the coherent scattering coupling g_2 in the absence (a) and presence (b) of the Coulomb interaction. E_m denotes the entanglement of two motional nanospheres, while E_{c1} (E_{c2}) represents the entanglement between the first (second) nanosphere and the cavity field. Other parameters are the same as those in Fig. 3.

By contrast, in Fig. 4(b) the entanglement E_m of two motional nanospheres could be generated via the Coulomb interaction either in the weak or ultra-strong optomechanical coupling regime. On the one hand, the Coulomb interaction provides the two-mode squeezing interaction ($\hat{b}_1^\dagger\hat{b}_2^\dagger$ and $\hat{b}_1\hat{b}_2$) on two nanospheres, which enables the entanglement of two nanospheres. On the other hand, with the state swapping due to the beam–splitter interaction ($\hat{b}_1^\dagger\hat{b}_2$ and $\hat{b}_1\hat{b}_2^\dagger$), entanglement E_{c1} and E_{c1} can be swapped via the Coulomb interaction.[22] Both E_{c1} and E_{c2} become stronger under the Coulomb interaction. When the coherent scattering coupling held at $g_1 = 0.3\Omega_1$, those entanglements rapidly drop to zero as the coherent scattering coupling g_2 increases to a critical point c. Here, the critical point c denotes the values of the coherent scattering couplings g_1 and g_2 as the entanglements drop to zero. Meanwhile, the system becomes unstable in this condition, which corresponds to the same critical point c in the boundary of the steady and unsteady regimes as shown in Fig. 3(b). We emphasize that the system being a steady state is a prerequisite for evaluating the entanglement via the logarithmic negativity (see Eqs. (7) and (8)). When the system is stable, the dynamics of the linear system in phase space is a point or a limit cycle in the long-time limit. Maximum entanglement can be achieved near the boundary of the steady and unsteady regimes.[39]

Based on the above discussion, the steady entanglement of two motional nanospheres could be induced via the Coulomb interaction. The two-mode squeezing interaction enhanced by the Coulomb interaction of two nanospheres will promote the generation of motional entanglement. The entanglement will increase with increase in the Coulomb interaction. On the other hand, the introduced Coulomb interaction disturbs the motion of each nanosphere, resulting in the instability of the system (comparing Figs. 3(a) and 3(b)). Therefore, there is the maximum entanglement in terms of the Coulomb interaction and system stability. Parameters (including charges, radius and distance of nanosphere) are chosen to achieve the maximum entanglement in a steady state.

Figure 5 shows the entanglement of two motional nanospheres E_m as a function of g_2 with different χ and d. With the increase (decrease) of χ (d), the Coulomb interaction is enhanced via the Coulomb coupling $G \propto \chi$ ($G \propto 1/d^3$). On the one hand, the enhancement of the Coulomb interaction can disturb the dynamics of the nanosphere, resulting in the instability of the system. On the other hand, the two-mode squeezing interaction will be improved. Therefore, E_m increases with increase (decrease) of χ (d) when the system parameters are selectively chosen to approach the unsteady state. Even for weak coherent scattering coupling, the entanglement of two nanospheres can be induced via the Coulomb interaction.

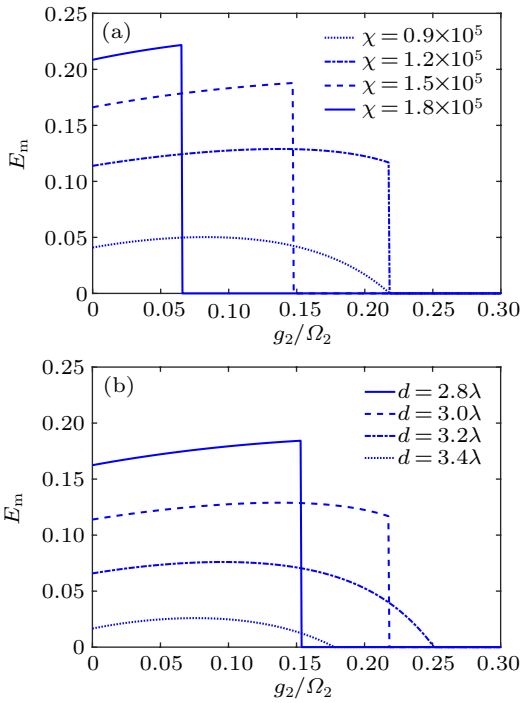


Fig. 5. Entanglement E_m of two motional nanospheres as a function of coherent scattering coupling g_2 with different χ (a) and d (b). The coherent scattering coupling between the first nanosphere and cavity field is given as $g_1 = 0.3\Omega_1$. Other parameters are the same as those in Fig. 3(b).

In order to achieve large entanglement of two nanospheres, the cavity decay rate κ and radius R_j of the nanosphere are also worth considering. Figure 6 shows $E_{\rm m}$ as a function of the cavity decay rate κ with different nanosphere radii R_j. With decrease of the radius R_j, the Coulomb coupling increases. In this condition, the system will be unstable if the cavity decay rate κ is low enough. $E_{\rm m}$ rapidly reaches a maximum as κ increases. Then $E_{\rm m}$ decreases with increase in κ because the cavity photons quickly decay to the vacuum. Even in the bad cavity limit $\kappa > \Omega_1$, $E_{\rm m}$ is available under the Coulomb interaction.

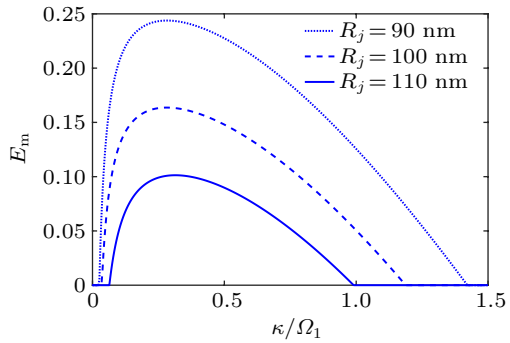


Fig. 6. Entanglement $E_{\rm m}$ of two motional nanospheres as a function of the cavity decay rate κ with different particle radii R_j. The coherent scattering couplings are assumed to be $g_1 = 0.1\Omega_1$ and $g_2 = 0.3\Omega_2$, respectively. Other parameters are the same as those in Fig. 3(b).

In our scheme, two nanospheres are optically levitated in the same cavity, and the gas molecules (or atoms) in the cavity are at room temperature. For the sake of convenience, two optically levitated nanospheres couple to the same thermal bath provided by collisions with the surrounding gas molecules (or atoms). The motional energy of the particle is comparable to that of the thermal fluctuations of the bath at room temperature $T_{\rm env} = T_{\rm a} = 300$ K.[29] In order to get rid of the decoherence due to gas molecule collisions, the nanosphere can be optically levitated in a high vacuum. However, with the reduction of gas molecule collisions in a high vacuum, the accumulated heat absorbed from the optical tweezers will amplify the thermal motion of the nanosphere, resulting in the instability of the system.[11] Therefore, it is very hard to optically levitate the nanosphere in a high vacuum. In order to generate the entanglement of two motional nanospheres in a steady state, cavity cooling is adopted to cool the two motional nanospheres from room temperature $T_{\rm env}$ to a low effective temperature T_j for CoM motion. Figure 7 shows $E_{\rm m}$ as a function of the effective temperature T_j of the jth nanosphere. In the presence of the Coulomb interaction, each of nanospheres is influenced not only by its own effective temperature but also by the effective temperature of the other nanosphere. The $E_{\rm m}$ induced by the Coulomb interaction has a distinctly fragile nature in the thermal environment. Cooling the CoM motion of the nanosphere to a low temperature could promote the generation of motional entanglement. By contrast to other similar schemes,[32–35] our solution does not require such stringent ground-state cooling and the motional entanglement can be generated in a few tens of mK, as shown in Fig. 7.

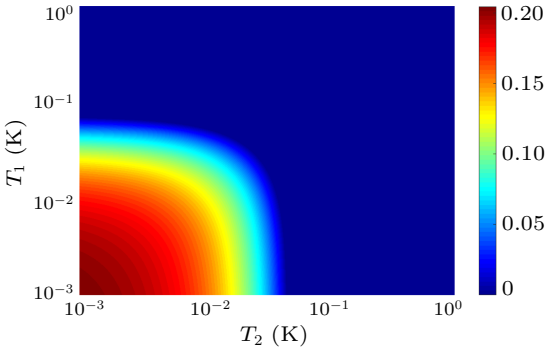


Fig. 7. Entanglement $E_{\rm m}$ of two motional nanospheres as a function of the effective temperature T_j. The coherent scattering couplings are assumed to $g_1 = 0.3\Omega_1$ and $g_2 = 0.15\Omega_1$, respectively. Other parameters are the same as those in Fig. 3(b).

5. Experimental feasibility

Based on the successful performance of the coherent scattering model, we proposed an implementable scheme to prepare the entanglement of two nanospheres in the presence of the Coulomb interaction.[20,26] However, a recent experiment has proved that the dipole–dipole coupling of two nanospheres can be of the order of the CoM motion.[26] In order to shut down the dipole–dipole interaction, the polarization of the optical tweezers needs to be manipulated.[26] With this, we can research the Coulomb interaction on two optically levitated nanospheres. Moreover, parameters in this context are all available from recent experiments and strong coupling and ultra-strong coupling have been observed.[18–21,26] According to the relationship between coherent scattering coupling and the phase of the cavity field, coherent scattering coupling can be manipulated by moving the position of the nanospheres within the cavity.[36] In this way, the coherent scattering coupling is flexible in the weak coupling, strong coupling, ultra-strong coupling and even deep-strong coupling regimes, as shown in Fig. 2. To consider system stability we could choose parameters in the regime of weak coupling, strong coupling or ultra-strong coupling.

The introduced Coulomb interaction has been widely applied in optical traps, demonstrating flexible control of the motion of levitated nanoparticles.[9,15,16,20,26] In general, an optically levitated nanoparticle can be positively ionized when the vacuum chamber is evacuated or carry charges via corona discharge.[41] Note that an optically levitated nanosphere is randomly charged. By driving the sinusoidal voltage signal of the electrodes close to the mechanical frequency, the charges can be assessed through phase measurement on the charged nanosphere.[26,41] The distance between two nanospheres can be accurately manipulated via acousto-optical deflectors, spa-

tial light modulators or other auxiliary setups such as piezoelectric actuators.[20,26]

In order to generate motional entanglement, two nanospheres could be optically levitated in a high-vacuum environment.[20,26,36] The lack of collisions between gas molecules and the nanospheres ultimately leads to dynamical instability.[11] Based on this, the motion of the optically levitated nanospheres should be reduced by cooling to a low temperature. Note that sympathetic cooling of two nanospheres near the ground state has been proven using laser cooling technology.[22] In that condition, the quality factor of a motional nanosphere can be higher than 10^8 if the residual gas pressure is of the order of 10^{-8} mba.[11] Based on the parameters in Fig. 3, the recoil heating rates from the gas molecule collisions and photon collisions are 1.1 kHz and 3.5 kHz, respectively (see Appendix C), which are smaller than the coherent scattering coupling of 32.6 kHz and Coulomb coupling of 24.9 kHz. This enables the motional entanglement of two nanospheres under the current experimental parameters.[14] We also adopt the logarithmic negativity to evaluate the entanglement.[14,40] In this way, the covariance matrix of two nanospheres can be constructed via the quantum tomography on two motional nanospheres.[8]

6. Conclusion

In summary, in this study we conducted a comprehensive analysis of quantum entanglement in a three-mode levitated optomechanical system in which two optically levitated nanospheres are simultaneously coupled to each other through the Coulomb interaction.[20,26] We found that quantum entanglement of two nanospheres can be induced in the presence of the Coulomb interaction regardless of whether the system is in the weak/strong coupling or ultra-strong coupling regime. Enhancing the Coulomb interaction by the charges, radii and distance of two nanospheres and cooling the CoM motion to the lower temperature, the entanglement of two nanospheres can be significantly improved. In order to achieve the maximum entanglement of two nanospheres, it is crucial for the dynamics of the system to approach the boundary between steady state and unsteady state, which can be accomplished by enhancing both the coherent scattering interaction and the Coulomb interaction. The engineered entanglement of multiple objects can be utilized to realize a matter-based quantum network to enhance the measurement precision of a matter-based quantum sensor network.[2–4]

Appendix A: Coulomb interaction

In the presence of Coulomb interaction, the Hamiltonian of two charged nanospheres can be written as[26]

$$\hat{H}_{\rm C} = \frac{k_{\rm e} Q_1 Q_2}{|d+\hat{y}_1-\hat{y}_2|}, \tag{A1}$$

where $k_{\rm e} = 1/(4\pi\varepsilon_0)$ is the electrostatic constant and d denotes the distance between two charged nanospheres. Expanding $\hat{H}_{\rm C}$ to the second order of $\hat{y}_{1,2}$, the effective Hamiltonian for the Coulomb interaction is given by

$$\hat{H}'_{\rm C} = \hbar G\left(\hat{b}_1^\dagger + \hat{b}_1\right)\left(\hat{b}_2^\dagger + \hat{b}_2\right), \tag{A2}$$

where $G = -\frac{Q_1 Q_2 y_0^1 y_0^2}{2\pi\varepsilon_0 d^3}$ is the induced Coulomb coupling between two charged nanospheres. Note that the operator $\hat{y}_{1,2}$ has been replaced by the phonon creation operator $(\hat{b}_{1,2}^\dagger)$ and annihilation operator $(\hat{b}_{1,2})$ via $\hat{y}_{1,2} = y_0^{1,2}\left(\hat{b}_{1,2}^\dagger + \hat{b}_{1,2}\right)$. $\hat{y}_0^{1,2}$ is the zero-point fluctuation amplitude of the charged nanosphere.

Appendix B: Damping in a rare gas

In a high vacuum, the mean free path of the gas molecules is much larger than the diameter of the spherical particles. The damping rate of a spherical particle in a rarefied gas can be numerically calculated by[42]

$$\gamma = \frac{6\pi\eta R}{m}\frac{0.619}{0.619+Kn}(1+c_K), \tag{B1}$$

where η and R (m) are the viscosity coefficient of the gas and the radius (mass) of the spherical particle. $Kn = l/R$ is the Knudsen number, where l is the mean free path of the gas molecules. $c_K = 0.31Kn/(0.785+1.152Kn+Kn^2)$ is a small positive function of Kn.

Appendix C: Recoil heating

The recoil heating from the residual gas molecules and photon collisions is given by[11,36]

$$\Gamma_{\rm gas} = \gamma\bar{n}, \tag{C1}$$

$$\Gamma_{\rm p} = \frac{\pi\varepsilon_0}{30\hbar}\left(\frac{\varepsilon_{\rm c} V E_0}{2\pi}\right)^2 k^5 y_0^2, \tag{C2}$$

where $\bar{n}$ is the occupation number and V is volume of the nanosphere. E_0 and y_0 are the amplitude of the tweezers and the zero-mean fluctuation of the nanosphere, respectively.

Acknowledgements

This research is supported by the National Natural Science Foundation of China (Grant No. 61771278) and the Beijing Institute of Technology Research Fund Program for Young Scholars.

References

[1] Graham T M, Song Y, Scott J, *et al.* 2022 *Nature* **604** 457
[2] Zhong Y, Chang H S, Bienfait A, *et al.* 2021 *Nature* **590** 571
[3] Abdi M, Pirandola S, Tombesi P and Vitali D 2012 *Phys. Rev. Lett.* **109** 143601

[4] Gilmore K A, Affolter M, Lewis-Swan R J, Barberena D, Jordan E, Rey A M and Bollinger J J 2021 *Science* **373** 673
[5] Liu X, Hu J, Li Z F, Li X, Li P Y, Liang P J, Zhou Z Q, Li C F and Guo G C 2021 *Nature* **594** 41
[6] Pompili M, Hermans S L, Baier S, *et al.* 2021 *Science* **372** 259
[7] Ritter S, Nölleke C, Hahn C, Reiserer A, Neuzner A, Uphoff M, Mücke M, Figueroa E, Bochmann J and Rempe G 2012 *Nature* **484** 195
[8] Kotler S, Peterson G A, Shojaee, Lecocq F, Cicak K, Kwiatkowski A, Geller S, Glancy S, Knill E, Simmonds R W, José A and John D T 2021 *Science* **372** 622
[9] Delić U, Reisenbauer M, Dare K, Grass D, Vuletić V, Kiesel N and Aspelmeyer M 2020 *Science* **367** 892
[10] Ranfagni A, Børkje K, Marino F and Marin F 2022 *Phys. Rev. Research* **4** 033051
[11] Jain V, Gieseler J, Moritz C, Dellago C, Quidant R and Novotny L 2016 *Phys. Rev. Lett.* **116** 243601
[12] Rahman A A and Barker P 2016 *Phys. Rev. A* **107** 013521
[13] Lepeshov S, Meyer N, Maurer P, Romero-Isart O and Quidant R 2023 *Phys. Rev. Lett.* **130** 233601
[14] Aspelmeyer M, Kippenberg T J and Marquardt F 2014 *Rev. Mod. Phys.* **86** 1391
[15] Tebbenjohanns F, Mattana M. L, Rossi M, Frimmer M and Novotny L 2021 *Nature* **595** 378
[16] Magrini L, Rosenzweig P, Bach C, Deutschmann-Olek A, Hofer S G, Hong S, Kiesel N, Kugi A and Aspelmeyer M 2021 *Nature* **595** 373
[17] Piotrowski J, Windey D, Vijayan J, Gonzalez-Ballestero C, de los Ríos Sommer A, Meyer N, Quidant R, Romero-Isart O, Reimann R and Novotny L 2023 *Nat. Phys.* **19** 1009
[18] de los Ríos Sommer A, Meyer N and Quidant R 2021 *Nat. Commun.* **12** 276
[19] Ranfagni A, Vezio P, Calamai M, Chowdhury A, Marino F and Marin F 2021 *Nat. Phys.* **17** 1120
[20] Vijayan J, Piotrowski J, Gonzalez-Ballestero C, Weber K, Romero-Isart O and Novotny L 2023 arXiv:2308.14721
[21] Dare K, Hansen J J, Coroli I, Johnson A, Aspelmeyer M and Delić U 2023 arXiv:2305.16226
[22] Penny T, Pontin A and Barker P 2023 *Phys. Rev. Research* **5** 013070
[23] Černotík O and Filip R 2020 *Phys. Rev. Research* **2** 013052
[24] Pettit R M, Ge W, Kumar P, Luntz-Martin D R, Schultz J T, Neukirch L P, Bhattacharya M and Vamivakas A N 2019 *Nat. Photonics* **13** 402
[25] Kuang T, Huang R, Xiong W, Zuo Y, Han X, Nori F, Qiu C W, Luo H, Jing H and Xiao G 2023 *Nat. Phys.* **19** 414
[26] Rieser J, Ciampini M A, Rudolph H, Kiesel N, Hornberger K, Stickler B A, Aspelmeyer M and Delić U 2022 *Science* **377** 987
[27] Zhu S C, Fu Z H, Gao X W, Li, C H, Chen Z M, Wang Y Y, Chen X F and Hu H Z 2023 *Photonics Res.* **11** 279
[28] Ahn J, Xu Z J, Bang J, Ju P, Gao X Y and Li T C 2020 *Nat. Nanotechnol.* **15** 89
[29] Millen J, Monteiro T S, Pettit R and Vamivakas A N 2020 *Rep. Prog. Phys.* **83** 026401
[30] Gonzalez-Ballestero C, Aspelmeyer M, Novotny L, Quidant R and Romero-Isart O 2021 *Science* **374** 3027
[31] Volpe G, Maragò O M, Rubinsztein-Dunlop H, *et al.* 2023 *J. Phys.: Photonics* **5** 022501
[32] Rudolph H, Hornberger K and Stickler B A 2020 *Phys. Rev. A* **101** 011804
[33] Brandão I, Tandeitnik D and Guerreiro T 2021 *Quantum Sci. Technol.* **6** 045013
[34] Weiss T, Roda-Llordes M, Torrontegui E, Aspelmeyer M and Romero-Isart O 2021 *Phys. Rev. Lett.* **127** 023601
[35] Rudolph H, Delić U, Aspelmeyer M, Hornberger K and Stickler B A 2022 *Phys. Rev. Lett.* **129** 193602
[36] Gonzalez-Ballestero C, Maurer Patrick, Windey Dominik, Novotny L, Reimann R and Romero-Isart O 2019 *Phys. Rev. A* **100** 013805
[37] Kockum A F, Miranowicz A, De Liberato S, Savasta S and Nori F 2019 *Nat. Rev. Phys.* **1** 19
[38] Leroux C, Govia L and Clerk A A 2018 *Phys. Rev. Lett.* **120** 093602
[39] Genes C, Mari A, Tombesi P and Vitali D 2008 *Phys. Rev. A* **78** 032316
[40] Vitali D, Gigan S, Ferreira A, Böhm H, Tombesi P, Guerreiro A, Vedral V, Zeilinger A and Aspelmeyer M 2007 *Phys. Rev. Lett.* **98** 030405
[41] Iwasaki M, Yotsuya T, Naruki T, Matsuda Y, Yoneda M and Aikawa K 2019 *Phys. Rev. A* **99** 051401
[42] Beresnev S A and Chernyak V G and Fomyagin G A 1990 *J. Fluid Mech.* **219** 405